

Supporting Information

Rational geometrical engineering of palladium sulphide multi-arm nanostructures as a superior bi-functional electrocatalyst

Ravi Nandan and Karuna K Nanda,

Materials Research Centre, Indian institute of Science, Bangalore-560012, India.

E-mail: nanda@mrc.iisc.ernet.in;

Fax: +91-80-2360 7316; Ph:+91-80-2293 2996

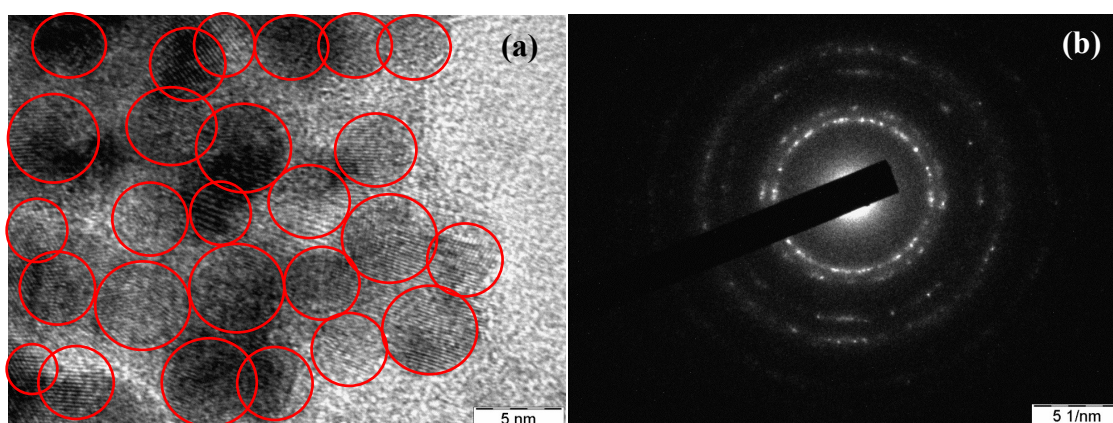


Fig. S1. (a,b) HRTEM image and SAED pattern for PSDNS-1.

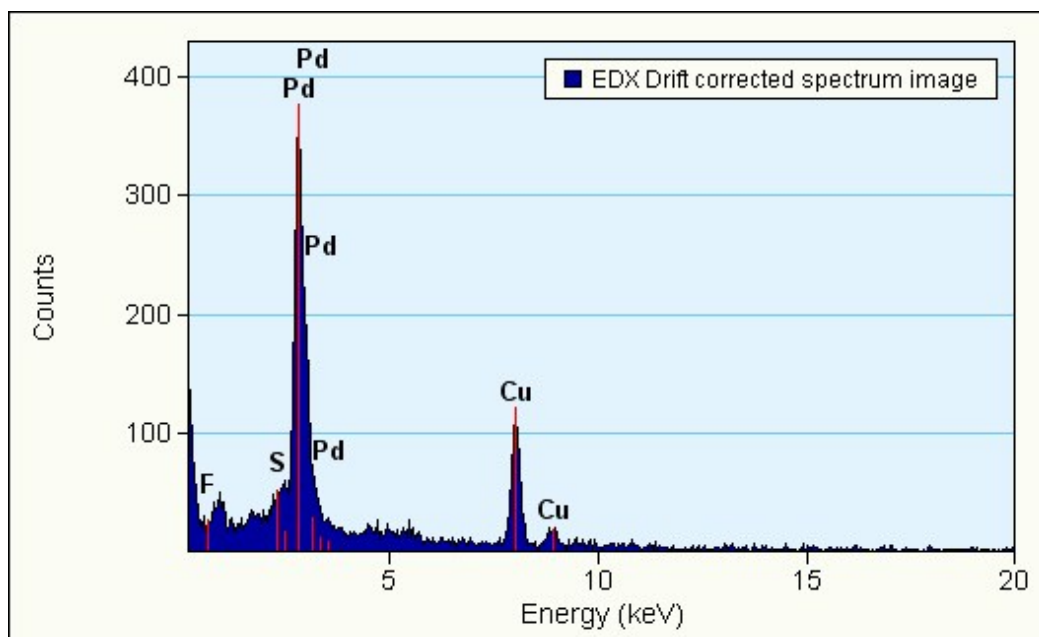


Fig. S2. EDS spectrum of PSDNS-1.

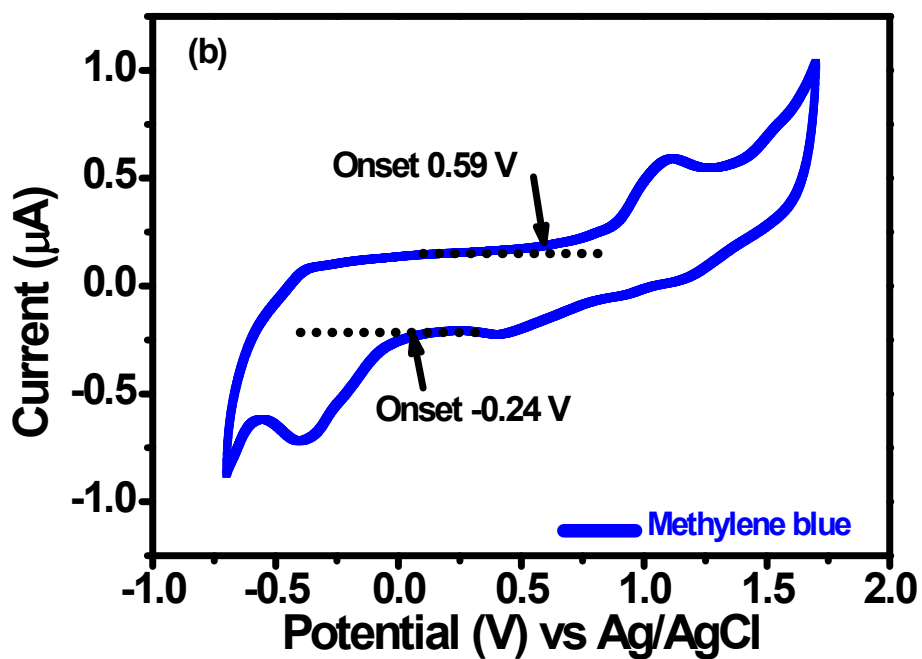
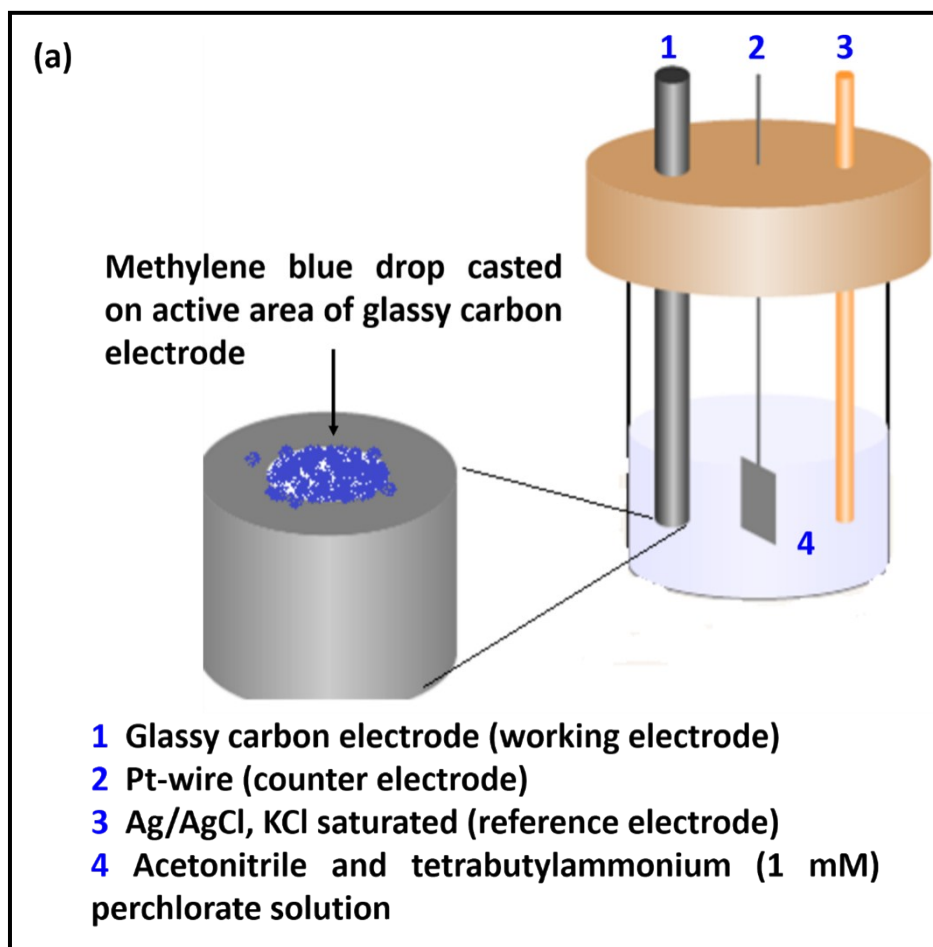


Fig. S3. (a) Schematic representation of three-electrode experimental set-up used for the evaluation of HOMO/LUMO levels of methylene blue (MB) using electrochemical technique. (b) Cyclic

voltammogram of MB in acetonitrile containing (1 mM) tetrabutylammonium perchlorate as the supporting electrolyte using traditional three electrode set-up at scan speed of 20 mV/s.

The HOMO and LUMO energy levels of MB were calculated using cyclic voltammogram. For this a traditional three-electrode set-up comprising of glassy carbon electrode (GCE, area $\sim 0.07 \text{ cm}^2$) coated with MB as the working electrode, KCl saturated Ag/AgCl as the reference electrode and platinum wire as the counter electrode. Experiment was carried in acetonitrile containing 1mM tetrabutylammonium perchlorate (used as received from Sigma Aldrich, purity $> 98 \%$) as the supporting electrolyte. The HOMO and LUMO energy levels in eV of MB were estimated using the following equations as reported in literature^{1,2}

$$E_{\text{HOMO}} = -e(E_{\text{oxd(onset)}} + 4.4) \quad (1)$$

$$E_{\text{LUMO}} = -e(E_{\text{red(onset)}} + 4.4) \quad (2)$$

where E_{oxd} ($\sim -0.59 \text{ V}$) and E_{red} ($\sim -0.24 \text{ V}$) represent the onset of oxidation and reduction potentials, respectively, obtained from CV recorded in acetonitrile at scan speed of 10 mV/s. The corresponding HOMO and LUMO levels calculated were -4.99 and -4.2 eV , respectively. HOMO of MB is 0.49 V above the potential of standard hydrogen electrode (SHE) and it is well above the reduction potentials of $[\text{PdCl}_4]^{2-}$ (0.591 V vs SHE), respectively.¹⁻³ The relative potentials level as discussed justify the possibility/plausibility of spontaneous reduction³ of palladium ions when mixed with MB solution.

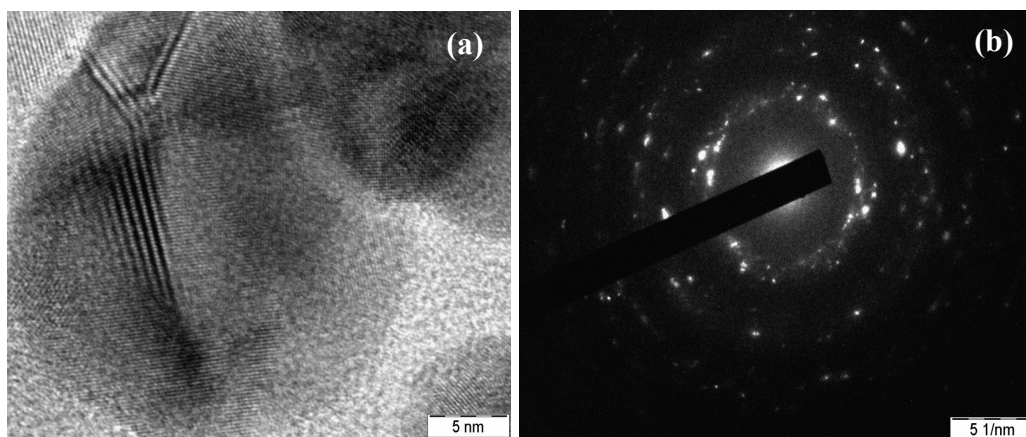


Fig. S4. (a,b)HRTEM image and SAED pattern for OPSDNS.

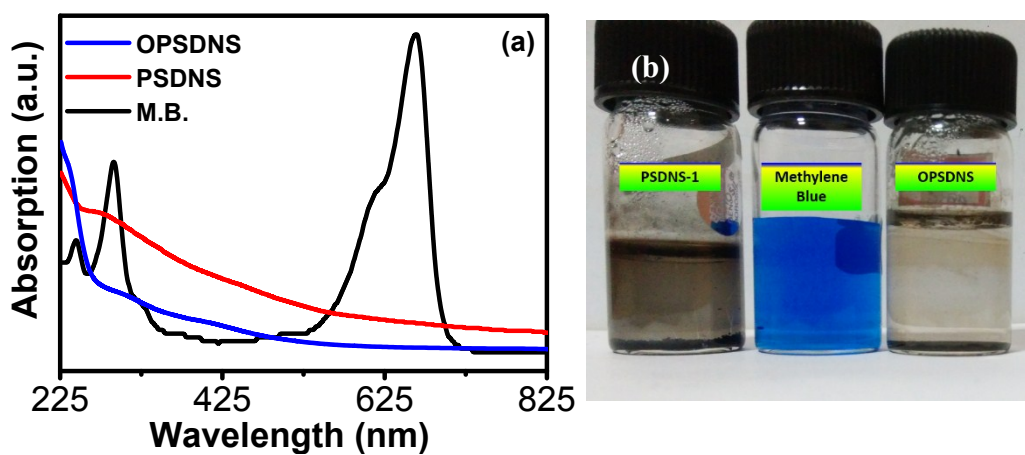


Fig. S5. (a)Absorbance spectrum and (b)optical photograph of methylene blue (M.B.), PSDNS-1 and OPSDNS in aqueous media.

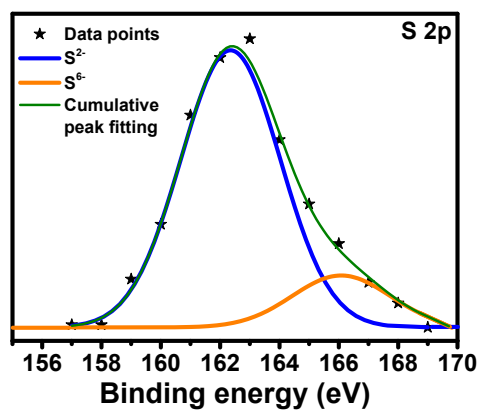


Fig. S6. Deconvulated core spectrum of S2p for OPSDNS.

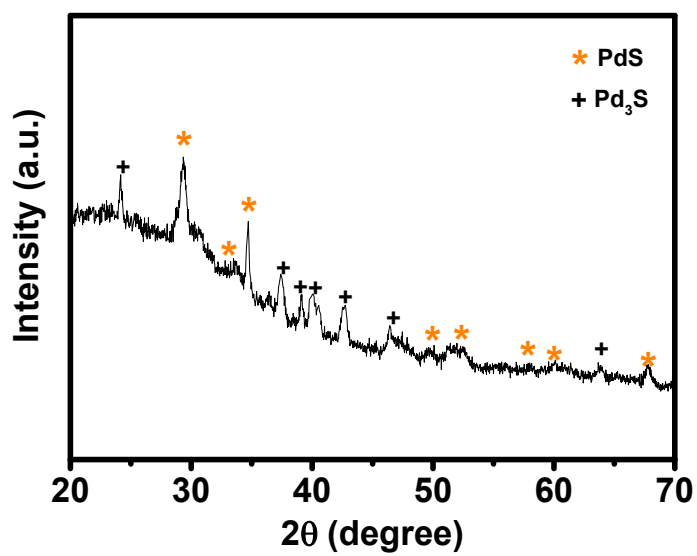


Fig. S7. X-ray diffraction pattern of OPSDNS.

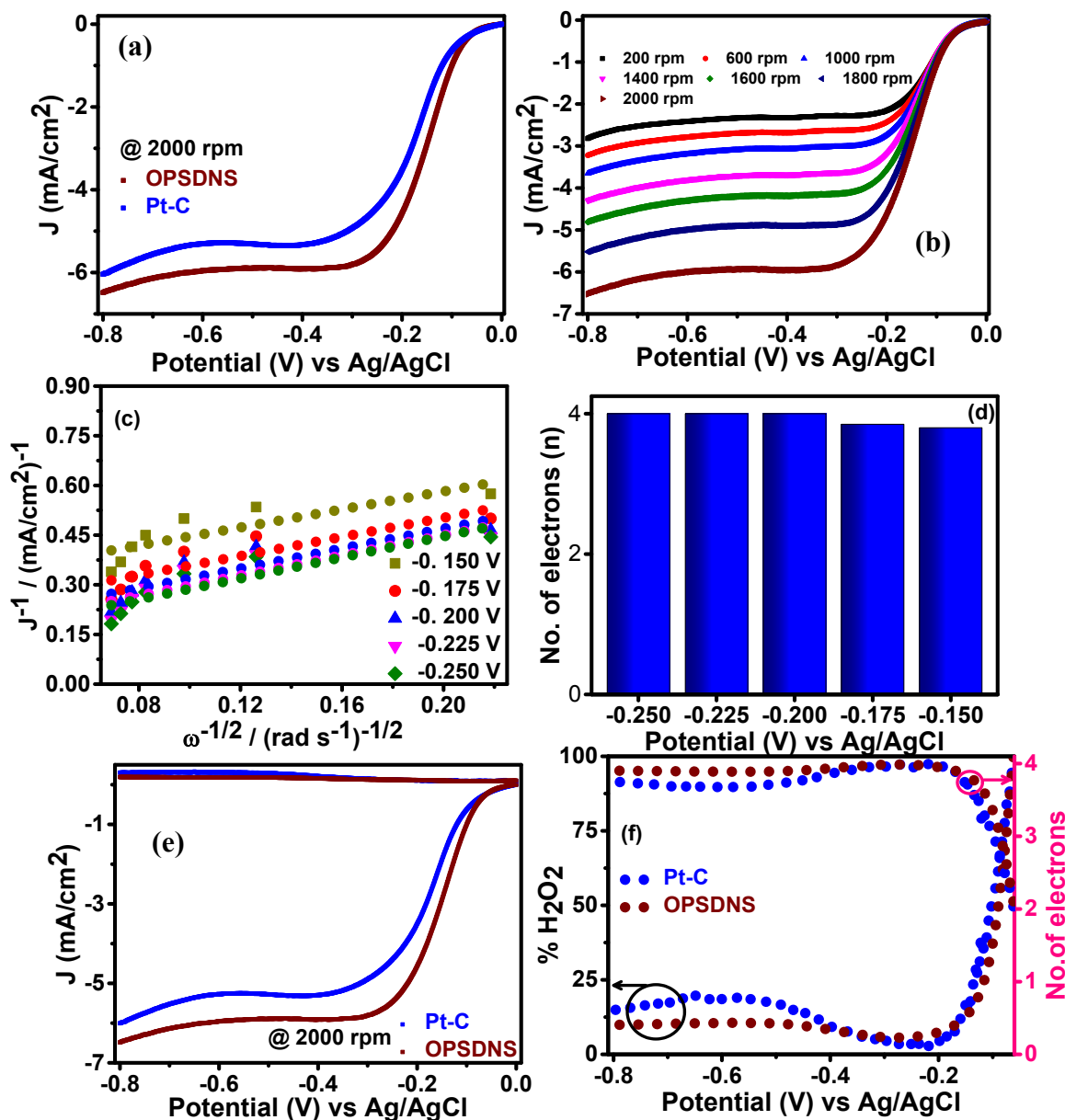


Fig. S8. (a) LSV-RDE curves for ORR on OPSDNS and Pt-C at 2000 rpm and at a scan rate of 10 mV/s. (b) LSV-RDE curves for ORR on OPSDNS at different electrode rotation speed at a scan rate of 10 mV/s. (c & d) corresponding Koutecky-Levich (K-L) plots and no. of electrons transfer for the ORR process on OPSDNS at different potentials in mixed controlled region deduced from figure (b). (e) RRDE voltammograms for OPSDNS and commercial Pt-C at 2000 rpm and scan rate of 10 mV/s, (f) percentage of peroxide formation and no. of electron transfer for ORR, deduced from figure (e). All measurements have been carried out in 0.1 M NaOH oxygen-saturated aqueous solution.

Figure S8a shows the RDE-LSV voltammograms for ORR process on Pt-C and OPSDNS in an oxygen-saturated aqueous alkaline (0.1M NaOH) solution at 2000 rpm and 10 mV/s scan rate. The E_{onset} for ORR obtained from RDE-LSV curve for OPSDNS and Pt-C is very much comparable (~ -35 mV). Remarkably, RDE-LSV voltammograms as shown in figure S8a suggests that the half-wave potential ($E_{1/2}$) and diffusion limited current density for OPSDNS are better with respect to Pt-C ($\Delta E_{1/2} \sim -30$ mV, $\Delta J_d \sim 0.6$ mA/cm² at 0.6 V vs Ag/AgCl). Figure S8b shows the RDE-LSV curves on OPSDNS at different rotation speeds and a scan rate of 10 mV/s in 0.1M NaOH solution. Alike to Pt-C (figure S8a), the current density plateaus for OPSDNS are well defined which is an indicative of uniform distribution of active sites in the catalyst under study. The voltammetric contours are similar to those obtained with Pt/Pt-alloy based electrocatalyst, where the ORR current density increases with increase of the rotation speeds due to availability of more oxygen flux at electrodes. The Koutecky–Levich (K-L) equation has been employed to evaluate the kinetic parameters of ORR in mixed control region. Figure S8c displays the K-L plots (J^{-1} vs. $\omega^{-1/2}$) at different electrode potentials. The good linear behaviour and parallel nature of lines (figure c) advocate the first order reaction kinetics for ORR on OPSDNS. The no. of electron transfer per oxygen molecule reduction is obtained from the slope of the K-L plots using K-L equation. It is evident from figure S8d that the ORR process on OPSDNS prominently follows the 4e⁻ pathway. Rotating ring-disk electrode (RRDE, with glassy carbon working electrode and Pt-ring electrode) study has also been carried out (fig. S8e) in 0.1M NaOH solution to monitor the peroxide (HO₂⁻) generation and no. of electron transfer number. Figure S8f shows the percentage of HO₂⁻ generation and the no. of electron transfer deduced from figure S8e. The percentage of HO₂⁻ generation on OPSDNS is ~ 10 and is less as compared to the percentage of HO₂⁻ generated on Pt-C catalyst under similar experimental conditions. It is evident from figure S8f that the reduction of oxygen on OPSDNS follow preferential 4e⁻ pathway and is in consort with the values obtained based on K-L plots (figure S8d).

Along with the current density, onset potential, half-wave potential, and Tafel slope also provide a measure of the catalytic efficiency of electrocatalyst. Theoretically, the Tafel slope for an ORR electrocatalyst in alkaline medium has been reported to be ~ 60 mV/dec in low overpotential and ~ 120 mV/dec in high overpotential region in ideal conditions. The Tafel slopes are ~ 69 and ~ 122 mV/dec (~ 81 and ~ 140 mV/dec) for OPSDNS (Pt-C) respectively in 1M NaOH solution. Tafel slopes obtained for OPSDNS in 0.1M NaOH solution are ~ 54 and ~ 114 mV/dec which is better than the values obtained for the Pt-C under similar conditions (as shown below) as well as to that in 1M NaOH solution. These results collectively advocate the better ORR activity of OPSDNS.

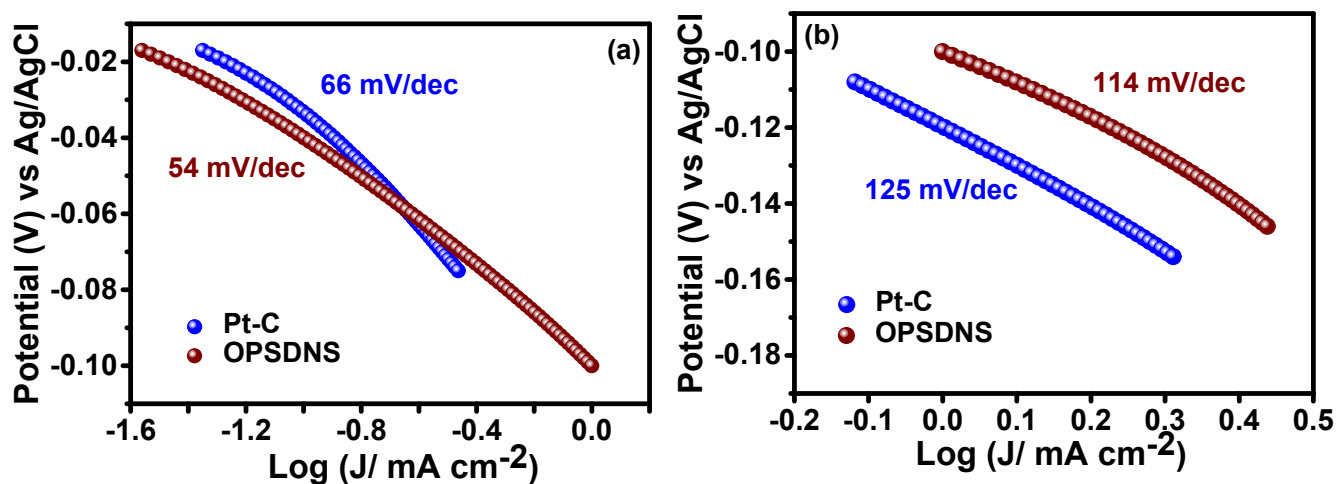


Fig. S9. Tafel slope calculation for ORR in 0.1M NaOH solution in (a) low over-potential region and (b) high over-potential regions on OPSDNS and Pt-C.

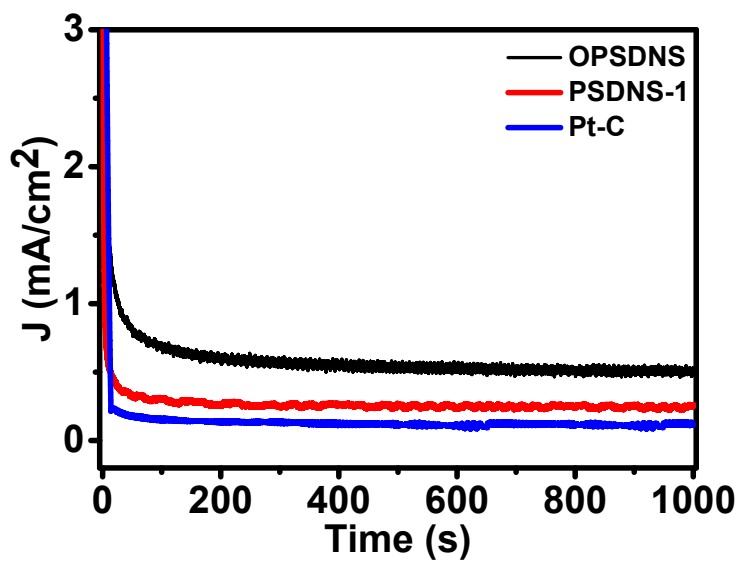


Fig. S10. Chronoamperometric study on OPSDNS, PSDNS-1 and Pt-C at -0.300 V in oxygen saturated alkaline medium.

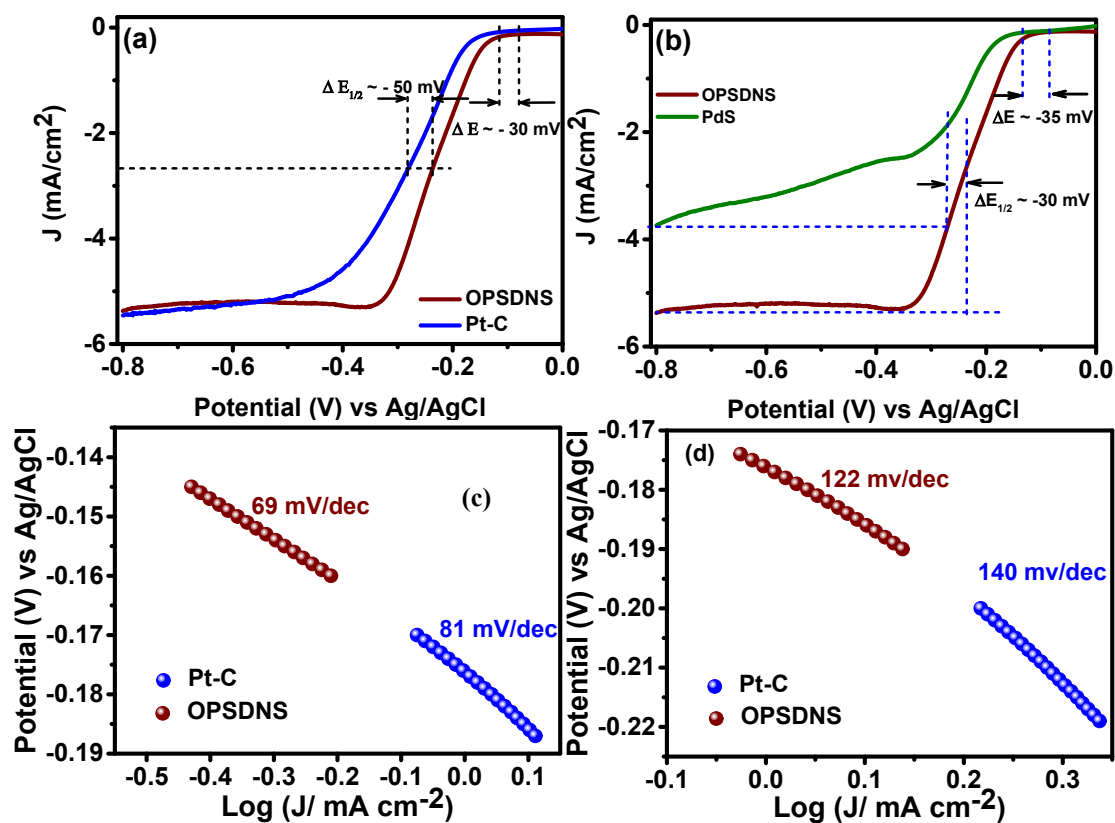


Fig. S11. (a,b) RDE-LSV ORR polarization curve at 2000 rpm and 10 mV/s scan speed in oxygen saturated alkaline aqueous medium for (a) Pt-C, OPSDNS and (b) PdS, OPSDNS. Tafel slope calculation in (c) low over-potential region and (d) high over-potential regions on OPSDNS and Pt-C.

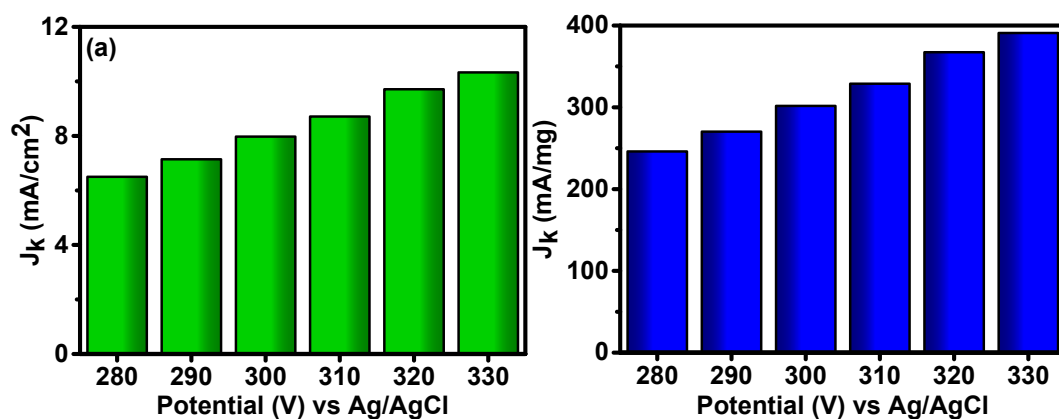


Fig. S12. (a,b) Normalized kinetic current (J_k) at different potential in mixed control region for ORR on OPSDNS in alkaline medium.

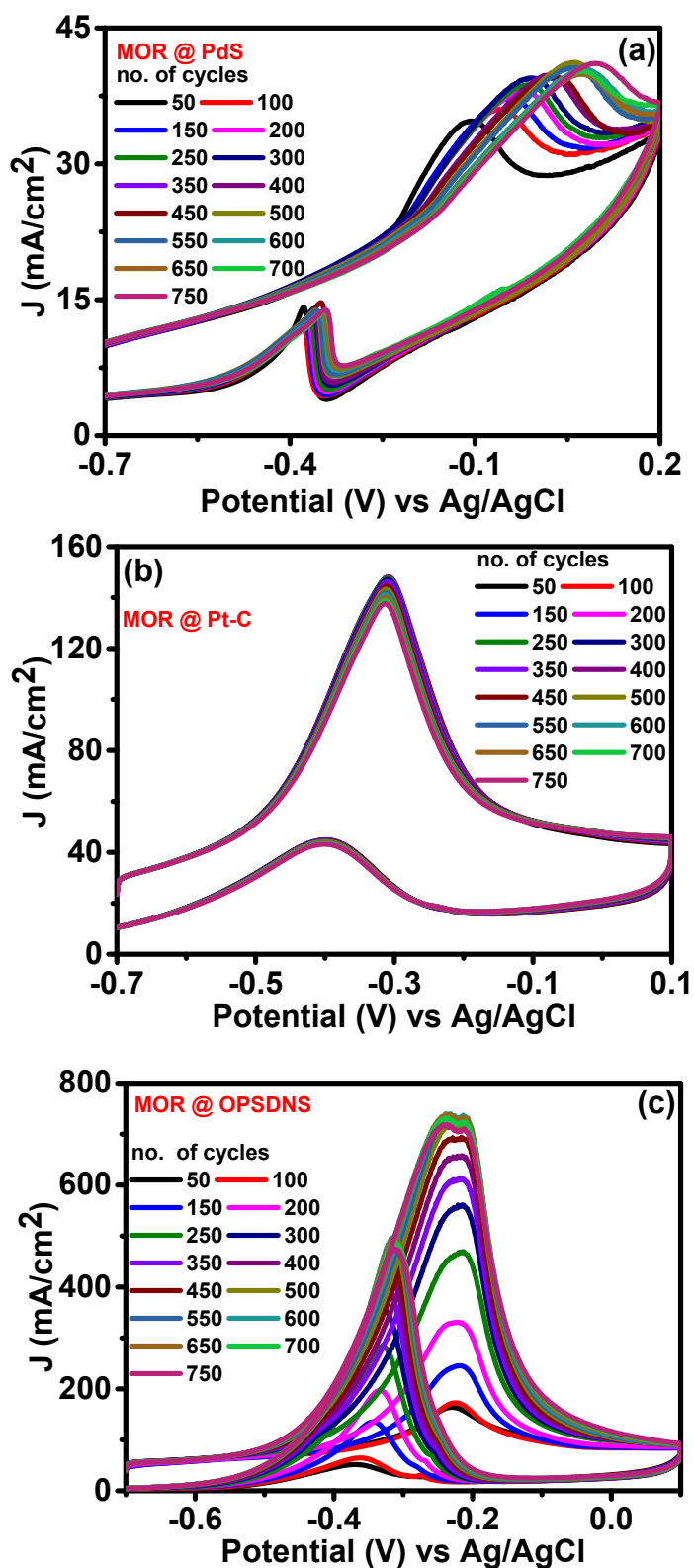


Fig. S13. (a-c) CV for electro-oxidation of methanol (0.5 M) in alkaline medium (1 M NaOH) at scan speed of 125 mV/s on PdS, Pt-C and OPSDNS.

Table S1. ORR activity of various noble metal based mono-/multi-component electro-catalysts.

Catalyst	Electrolyte	E_{on-set} (V) (Vs Ag/AgCl)	$E_{1/2}$ (V) (Vs Ag/AgCl)	Reference
Ag-Ptnanocube	0.1 M NaOH	-0.105	-0.275	International Journal of Hydrogen Energy 39 (2014) 5528-5536
Ag-Pt-Ag nanocube	0.1 M NaOH	-0.095	-0.275	International Journal of Hydrogen Energy 39 (2014) 5528-5536
Au cluster/rGO composite	0.1 M KOH	-0.125	-0.310	J. Mater. Chem. A 2014, 2, 13682-13690
Au nanocluster	0.1 M KOH	-0.100	-0.275	Angew. Chem. Int. Ed. 48 (2009) 4386-4389.
Au/rGOnanocomposite	0.1 M KOH	-0.230	-0.475	Adv. Funct. Mater. 2014, 24, 2764-2771
Au-3 nm cluster	0.5 M KOH	-0.150	-0.650	J. Phys. Chem. C 2008, 112, 10515-10519
Au-7 nm cluster	0.5 M KOH	-0.200	-0.730	J. Phys. Chem. C 2008, 112, 10515-10519
Pt-Au-PyG	0.1 M KOH	-0.060	-0.325	ACS Appl. Mater. Interfaces 2014, 6,13448-13454
Pt-Au-PyNG	0.1 M KOH	-0.100	-0.405	ACS Appl. Mater. Interfaces 2014, 6,13448-13454
Au NPs/GCE	0.1 M KOH	-0.270	-----	Electrochemistry Communications 38 (2014) 82-85
Au NPs-rGO/GCE	0.1 M KOH	-0.100	-0.375	Electrochemistry Communications 38 (2014) 82-85
Au NPs/rGO	0.1 M KOH	-0.180	-0.445	ACS Appl. Mater. Interfaces 2013, 5, 654-662
Pt-C	0.1 M KOH	-0.130	-0.400	Electrochim. Acta 2014, 133, 407-413.
Pd-C	1 M KOH	-0.240	-0.307	Langmuir 2012, 28, 7168-7173
Au@Pd	1 M KOH	-0.220	-0.303	Langmuir 2012, 28, 7168-7173
G-CuPd ₄ NCPs	0.1 M KOH	-0.105	-0.335	ACS Appl. Mater. Interfaces 2015, 7, 5347-5357
G-CuPd NCPs	0.1 M KOH	-0.105	-0.305	ACS Appl. Mater. Interfaces 2015, 7, 5347-5357
AgPd ₂	0.1 M KOH	-0.099	-0.205	J. Am. Chem. Soc. 2012, 134, 9812-9819
Ag ₂ Pd	0.1 M KOH	-0.099	-0.240	J. Am. Chem. Soc. 2012, 134, 9812-9819
Ag ₄ Pd	0.1 M KOH	-0.099	-0.240	J. Am. Chem. Soc. 2012, 134, 9812-9819
Ag ₉ Pd	0.1 M KOH	-0.099	-0.274	J. Am. Chem. Soc. 2012, 134, 9812-9819
Pdnanocube (~ 63 nm)	1 M NaOH	-0.100	-0.250	International Journal of Hydrogen Energy 37 (2012) 3993-3997
heteroatom-doped carbon-Pd nanostructure	0.1 M NaOH	-0.110	-0.350	Nano Energy (2015) 12, 33-42
Pt-C (20 % Pt loading)	1 M NaOH 0.1M NaOH	-0.125 -0.035	-0.287 -0.185	Present Study
PdS (Commercial)	1 M NaOH	-0.142	-0.260	Present Study
PSDNS1	1 M NaOH	-0.125	-0.263	Present Study
OPSDNS	1 M NaOH 0.1M NaOH	-0.095 -0.035	-0.237 -0.160	Present Study

Table S2. Mass activity for methanol electro-oxidation in alkaline media using various mono-/multi-metallic catalysts.

Catalyst composition	Testing conditions	Mass activity	Ref.
Pt/Y-zeolite (Y)/Vulcan XC-72R	0.1 M KOH and 1 M CH ₃ OH, 100 mVs ⁻¹	7 mA mg ⁻¹	<i>RSC Adv</i> 2015 , <i>5</i> , 7637-7646.
Pt/ceria nano rods	0.5 M KOH and 1 M CH ₃ OH, 100 mVs ⁻¹	25 mA mg ⁻¹	<i>RSC Adv</i> 2014 , <i>4</i> , 1270-1275.
Pt-Sn	1 M KOH and 1 M CH ₃ OH, 10 mVs ⁻¹	100 mA mg ⁻¹	<i>Electrochim Acta</i> 2009 , <i>54</i> , 989-995.
Pd/Fe ₃ O ₄ /GC	0.1 M NaOH and 1 M CH ₃ OH 50 mVs ⁻¹	110 mA mg ⁻¹	<i>Mater. Sci. Eng., B</i> 2010 , <i>172</i> , 207-212.
Pd/SnO ₂ -TiO ₂ /MWCNT	0.5 M NaOH and 1 M CH ₃ OH, 20 mVs ⁻¹	114 mA mg ⁻¹	<i>Electrochim Acta</i> 2013 , <i>102</i> , 79-87.
Pt-on-Pd-on-Au/CNTs	1 M NaOH and 1 M CH ₃ OH, 50 mVs ⁻¹	147 mA mg ⁻¹	<i>Electrochim Acta</i> 2014 , <i>148</i> , 1-7.
Pt/G-V(C, N)	1 M KOH and 2 M CH ₃ OH, 50 mVs ⁻¹	210 mA mg ⁻¹	<i>Nanoscale</i> 2015 , <i>7</i> , 1301-1307.
CuxPdy/C	0.5 M KOH and 0.5 M CH ₃ OH, 50 mVs ⁻¹	220 mA mg ⁻¹	<i>Electrochim Acta</i> 2015 , <i>174</i> , 1-7.
np-Pd	1 M KOH and 0.5 M CH ₃ OH, 10 mVs ⁻¹	223.52 mA mg ⁻¹	<i>J. Power Sources</i> 2010 , <i>195</i> , 6740-6747.
Pd-NiO/C	1 M KOH and 1 M CH ₃ OH, 10 mVs ⁻¹	250 mA mg ⁻¹	<i>Electrochim Acta</i> 2013 , <i>90</i> , 108-111.
Pd/graphene	0.5 M NaOH and 1 M CH ₃ OH, 50 mVs ⁻¹	283 mA mg ⁻¹	<i>J. Mater. Chem</i> 2012 , <i>22</i> , 22533-22541.
Pd/PPY/graphene	0.5 M NaOH and 1 M CH ₃ OH, 50 mVs ⁻¹	359.8 mA mg ⁻¹	<i>Electrochim Acta</i> 2011 , <i>56</i> , 1967-1972.
PdMo/CNT	1 M KOH and 1 M CH ₃ OH, 50 mV s ⁻¹	395.6 mA mg ⁻¹	<i>Int. J. Hydrogen. Energy</i> 2012 , <i>37</i> , 19055-19064.
PdCuSn/CNTs	1 M KOH and 0.5 M CH ₃ OH, 50 mVs ⁻¹	395.94 mA mg ⁻¹	<i>J. Power Sources</i> 2013 , <i>242</i> , 610-620.
Pt/WO ₃ /MC	0.5 M NaOH and 1 M CH ₃ OH, 25 mVs ⁻¹	410 mA mg ⁻¹	<i>Electrochim Acta</i> 2013 , <i>94</i> , 80-91.
Pd/MnO ₂ /CNT	0.5 M NaOH and 1 M CH ₃ OH, 50 mVs ⁻¹	432.02 mA mg ⁻¹	<i>Int. J. Hydrogen. Energy</i> 2010 , <i>35</i> , 10522-10526.
PtNi/POMA/GE/GC	1 M KOH and 1 M CH ₃ OH, 50 mVs ⁻¹	520.5 mA mg ⁻¹	<i>RSC Adv</i> 2014 , <i>4</i> , 24156-24162.
PtNi/C	1 M NaOH and 1 M CH ₃ OH, 50 mV s ⁻¹	559 mA mg ⁻¹	<i>J. Phys. Chem C</i> 2010 , <i>114</i> , 19714-19722.
PdNi/C	1 M KOH and 1 M CH ₃ OH, 50 mVs ⁻¹	575 mA mg ⁻¹	<i>Electrochem. Commun</i> 2009 , <i>11</i> , 925-928.
Pt-PdCo/P-MWCNTs	0.1 M KOH and 1 M CH ₃ OH, 20 mVs ⁻¹	575 mA mg ⁻¹	<i>Electrochem. Commun</i> 2011 , <i>13</i> , 886-889.
Ti ₃₀ Cu ₆₀ Pd ₁₀	0.5 M NaOH and 1 M CH ₃ OH, 25 mVs ⁻¹	577.85 mA mg ⁻¹	<i>J. Electrochem. Soc</i> 2014 , <i>161</i> , F1474-F1480.
PtAu/PDA-RGO	1 M KOH and 1 M CH ₃ OH, 50 mVs ⁻¹	645.1 mA mg ⁻¹	<i>Electrochim Acta</i> 2015 , <i>153</i> , 175-183.
Pd/TiO ₂ -C	0.5 M KOH and 1 M CH ₃ OH, 5 mVs ⁻¹	650 mA mg ⁻¹	<i>Electrochim Acta</i> 2013 , <i>112</i> , 164-170.
Pd and N-CNPs Nanodendrite	1 M NaOH and 1 M CH ₃ OH, 50 mVs ⁻¹	653 mA mg ⁻¹	<i>Green Chem.</i> 2016 , DOI: 10.1039/c5gc02508g
PdS	1 M NaOH and 1 M CH ₃ OH, 125 mVs ⁻¹	41 mA mg ⁻¹	Present Study
Pt-C (20% Pt loading)	1 M NaOH and 1 M CH ₃ OH, 125 mVs ⁻¹	138 mA mg ⁻¹	Present Study
OPSDNS	1 M NaOH and 1 M CH ₃ OH, 125 mVs ⁻¹	715mA mg ⁻¹	Present Study

References

1. V. Gupta, N. Chaudhary, R. Srivastava, G. Datt Sharma, R. Bhardwaj and S. Chand, *J. Am. Chem. Soc.*, 2011, 133, 9960.
2. R. Nandan and K. K. Nanda, *J. Mater. Chem. A* 2017,10.1039/C7TA02293J.
3. H. C. Choi, M. Shim, S. Bangsaruntip and H. Dai, *J. Am. Chem. Soc.* ,2002, 124, 9058.